Rhodium-oxide-coated indium tin oxide for enhancement of hole injection in organic light emitting diodes

Soo Young Kim, Jeong Min Baik, Hak Ki Yu, Kwang Young Kim, Yoon-Heung Tak, and Jong-Lam Lee

Articles you may be interested in

Efficient and reliable green organic light-emitting diodes with Cl2 plasma-etched indium tin oxide anode
J. Appl. Phys. **112**, 013103 (2012); 10.1063/1.4731713

Stabilization of the work function of indium tin oxide using organic surface modifiers in organic light-emitting diodes
Appl. Phys. Lett. **93**, 163308 (2008); 10.1063/1.2998599

Enhancement of hole injection using ozone treated Ag nanodots dispersed on indium tin oxide anode for organic light emitting diodes
Appl. Phys. Lett. **90**, 163516 (2007); 10.1063/1.2719153

Enhancement of hole injection using iridium-oxide-coated indium tin oxide anodes in organic light-emitting diodes
Appl. Phys. Lett. **86**, 133504 (2005); 10.1063/1.1894605

Enhancement of hole injection using O 2 plasma-treated Ag anode for top-emitting organic light-emitting diodes
Appl. Phys. Lett. **86**, 012104 (2005); 10.1063/1.1846149

Rhodium-oxide-coated indium tin oxide for enhancement of hole injection in organic light emitting diodes

Soo Young Kim, Jeong Min Baik, and Hak Ki Yu
Department of Materials Science and Engineering, Pohang University of Science and Technology (POSTECH), Pohang, Kyungbuk 790-784, Korea

Kwang Young Kim and Yoon-Heung Tak
LG Electronics Inc., Kumi, Kyungbuk, 730-030, Korea

Jong-Lam Lee[a)]
Department of Materials Science and Engineering, Pohang University of Science and Technology (POSTECH), Pohang, Kyungbuk 790-784, Korea

The authors report the enhancement of hole injection using an RhO_x layer between indium tin oxide anodes and 4,4′-bis[N-(1-naphtyl)-N-phenyl-amino]biphenyl in organic light-emitting diodes (OLEDs). The operation voltage of OLEDs at 700 cd/m^2 decreased from 13 to 10 V as the Rh layer changed to RhO_x by surface treatment using O_2 plasma. Synchrotron radiation photoelectron spectroscopy results showed that the work function increased by 0.2 eV as the Rh layer transformed into RhO_x. Thus, the hole injection energy barrier was lowered, reducing the turn-on voltage and increasing the quantum efficiency of OLEDs. © *2005 American Institute of Physics.*
[DOI: 10.1063/1.2012534]

Ever since the high efficiency organic light-emitting diodes (OLEDs) were reported, numerous efforts have been made to improve OLED characteristics. The performance of an OLED is influenced by the properties of the injecting electrodes and the electrode-organic interfaces.[1] The potential barrier between electrodes and organic layers exists due to the energy level difference. The barrier for electron injection subsequently reduced using electron injection promoters, such as lithium and cesium fluorides.[2,3] At the interface of an indium tin oxide (ITO) anode with organic materials, enhanced hole injection was also desired to increase internal quantum efficiency by balancing charge carriers in the active layer. One of the most well-known approaches for reducing potential barriers for hole injection is the elevation of work function of ITO anodes.[4–6] Several approaches for achieving an elevated ITO work function have been performed to modify its surface chemical states, including surface plasma treatment, the insertion of metal oxides with a high work function between ITO and organic material, and the formation of a metal-doped indium tin oxide layer on an ITO surface.[6–8] Rhodium oxide (RhO_x) is a transparent conducting oxide. The work function of RhO_x(~5.0 eV) is higher than that of ITO (~4.7 eV).[9] Thus, it is expected that the interfacial layer of RhO_x between ITO anodes and organic materials could improve the injection of holes via enhanced OLED electrical properties.

In this letter, we report the enhancement of electrical and optical performance of OLEDs by using an interfacial layer of RhO_x between ITO anodes and the hole transport layer of 4′-bis[N-(1-naphtyl)-N-phenyl-amino]biphenyl (α-NPD). The RhO_x layer was prepared by exposing a thin Rh layer to O_2 plasma. The x-ray reflectivity method was used to examine the thickness of the thin Rh layer and relative roughness. The change in work function with the formation of RhO_x was

examined using synchrotron radiation photoelectron spectroscopy (SRPES). From this, the effects of RhO_x layers on the enhancement of both electrical and optical properties of OLEDs were discussed.

A glass coating with ITO (150 nm thick, ~20 Ω/□) was used as the starting substrate. The ITO surface was cleaned in sequence with acetone, isopropyl alcohol and deionized water, and then dried with a high purity nitrogen gas. The ITO surface was treated with O_2 plasma for 1 min under 100 mTorr ("ITO"). The plasma power was 150 W. A thin layer of Rh with a thickness of 2 nm was deposited on the plasma-treated ITO by an *e*-beam evaporator ("Rh/ITO"). The Rh film was also exposed to the O_2 plasma for 1 min to produce a RhO_x layer ("O_2-Rh/ITO"). The thickness of the thin layer was deduced from the period of the oscillations in x-ray reflection, measured at the 3C2 beamline of the Pohang Acceleration Laboratory (PAL). These three types of samples were loaded into a thermal evaporator and α-NPD with a thickness of 70 nm, tris(8-hydroxyquinoline) aluminum (Alq$_3$, 60 nm), and aluminum (Al, 150 nm) layers were deposited in sequence. During deposition, the base pressure of the chamber was maintained as low as 10^{-6} Torr. The active area of the device was 3×3 mm^2. The current density-voltage and luminescence-voltage characteristics of the devices were measured. The surface treatment conditions for the three kinds of anodes are summarized in Table I.

X-ray reflectivity was used to measure the exact thickness of the Rh layer and Rh surface morphology. In order to

TABLE I. Anode preparation methods for OLEDs.

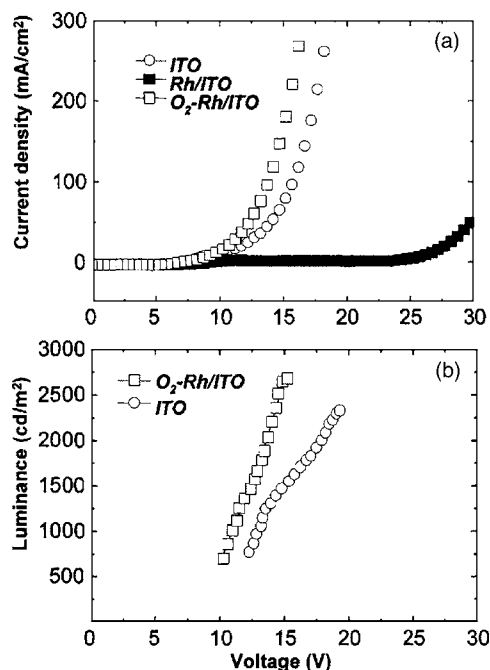|	OLED anodes
ITO	ITO+O$_2$ plasma treatment
Rh/ITO	ITO+O$_2$ plasma treatment + Rh deposition
O$_2$-Rh /ITO	ITO+O$_2$ plasma treatment + Rh deposition + O$_2$ plasma treatment

[a)]Electronic mail: jllee@postech.ac.kr

FIG. 1. (a) Current density-voltage and (b) luminance-voltage characteristics of OLEDs with different anodes.

FIG. 2. X-ray reflectivity data of O$_2$-Rh/ITO and Rh/ITO.

investigate the chemical bonding states of ITO by inserting the RhO$_x$ interfacial layer, the three samples were loaded into a vacuum chamber, equipped with an electron analyzer, at the PAL 4B1 beamline. An incident photon energy of 650 eV was used to obtain Rh $3d$, In $3d$, Sn $3d$, O $1s$, and C $1s$ core level spectra. The onset of photoemission, corresponding to the vacuum level at the ITO surface, was measured with a negative bias (-20 V) on the sample to avoid the work function of the detector. The incident photon energy was calibrated with the core level spectrum of Au $4f$.

Figure 1(a) shows the current density-voltage characteristics of the three types of devices. The turn-on voltage increased from 7 to 25 V when the 2 nm thick Rh was deposited on ITO. However, it was drastically decreased to 5 V as the Rh layer was treated with O$_2$ plasma. The decrease in turn-on voltage is a reflection of improved hole injection efficiency. Luminance-voltage curves are shown in Fig. 1(b). The operation voltage corresponding to 700 cd/m^2 was 13 V for ITO and 10 V for O$_2$-Rh/ITO. The external quantum efficiencies at 700 cd/m^2 are calculated at 1.1% for O$_2$-Rh/ITO and 0.34% for ITO, respectively. The electroluminescence spectra of the Rh/ITO sample could not be measured using our optical system because its intensity was very low. It is thought that holes were effectively injected from an anode to an organic layer, promoting internal quantum efficiency.

Figure 2 shows the x-ray reflectivity curves of Rh/ITO and O$_2$-Rh/ITO samples. The thickness of the Rh layer estimated from the x-ray reflectivity data was 2 nm. The film thickness is given by $2\pi/\Delta q$, where Δq is the period of the intensity oscillations in the reflectivity curves.[10] The amplitude of the intensity oscillation in the O$_2$-Rh/ITO sample is higher than that in the Rh/ITO sample. The intensity oscillation reflects the interference pattern of x rays reflected from the surface and the interface. Therefore, it is considered that the Rh surface became smoother after O$_2$ plasma treatment.
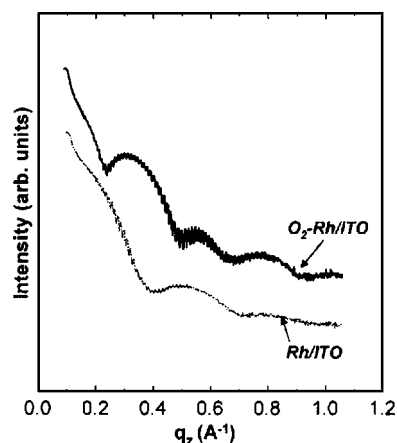
Figure 3(a) shows O $1s$ SRPES spectra for three kinds of samples. In order to separate the chemical bonding states including those in the spectra, the spectral line shape was simulated using a suitable combination of Gaussian and Lorentzian functions. The O $1s$ peak was separated into two components. The P1 peak centered at 532.2 eV in ITO was due to residual surface contaminants.[11] The P2 peak centered at 530 eV was assigned to O^{2-} ions in the tetrahedral interstices of face-centered cubic In^{3+} ion arrays.[12] In the case of Rh/ITO, the peak intensity of O $1s$ decreased. The photoemission flux I_d penetrating a film decreased exponentially with the increase of thickness d, expressed as $I_d = I_0 \exp(-d/\lambda)$, where I_0 is the flux emitted by the clean backing material and λ is the inelastic mean-free path of an electron traveling within a solid.[13] The reduction of O $1s$ peak intensity in the Rh/ITO is due to the exponential decrease of photoemission flux. In O$_2$-Rh/ITO, a new P3 peak centered at 529.5 eV appeared, indicating the O-Rh bond. Therefore, it is thought that O$_2$ plasma treatment transformed the Rh layer into a transparent RhO$_x$ layer. The Rh $3d$ core level spectra of Rh/ITO and O$_2$-Rh/ITO are shown in Fig. 3(b). The Rh $3d_{5/2}$ and Rh $3d_{3/2}$ peaks shifted about 1.5 eV toward a higher binding energy after O$_2$ plasma treatment. It is reported that the binding energy of the Rh-O bond is 1.4 ~1.6 eV higher than that of the Rh-Rh bond.[14] Thus, the shift of Rh $3d_{5/2}$ and Rh $3d_{3/2}$ peaks is due to the formation of RhO$_x$ layers.

The relative change of the work function was measured using secondary electron emission spectra, as shown in Fig.
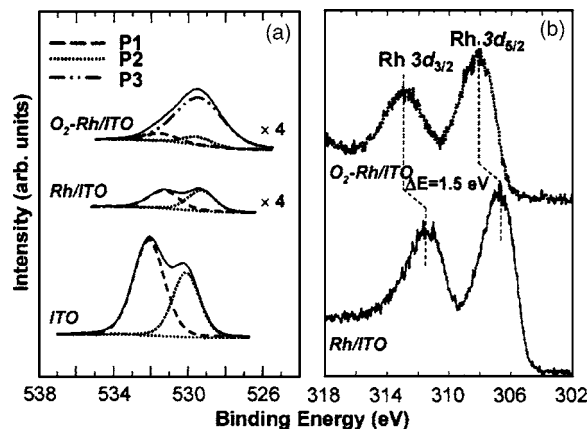

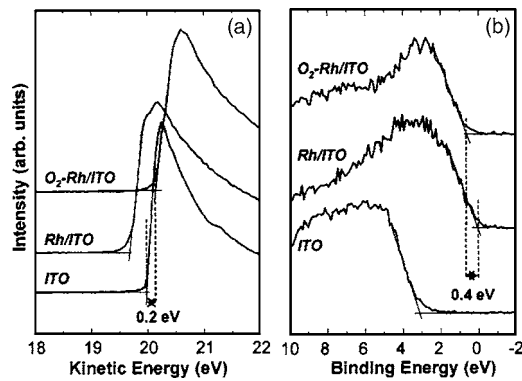FIG. 3. (a) O $1s$ and (b) Rh $3d$ core level spectra for three kinds of anodes.

FIG. 4. (a) Secondary electron-emission spectra and (b) relative change of valence band maximum for the samples.

4(a). The onset of secondary electrons was determined by extrapolating two solid lines from the background and straight onset in the spectra.[15] The onset of a secondary electron for O_2-Rh/ITO shifted to the higher kinetic energy by 0.2 eV with respect to the onset for ITO. This result means that the work function of RhO_x-coated ITO is higher by 0.2 eV than that of O_2 plasma-treated ITO. Figure 4(b) shows the relative change in the valence band maximum (VBM) with the formation of a RhO_x layer. The VBM was calibrated with a clean Au surface. The VBM at the ITO surface is located 3.0 eV apart from the Fermi level. After the Rh layer deposition on the ITO surface, the VBM of Rh/ITO coincided with the Fermi level, showing the metallic valance band. However, the VBM of O_2-Rh/ITO is located at 0.4 eV, apart from the Fermi level. This means that the bandgap was produced due to the formation of RhO_x. This is in good agreement with the result of Fig. 3.

Based on these experimental observations, the reduction in operation voltage could be explained as later. The electron concentration of ITO is about 10^{20}–10^{21} cm^{-3}.[16] Thus, the Fermi level of ITO is close to the conduction band maximum due to its high electron concentration. After O_2 plasma treatment, surface band bending increased, as shown in Fig. 5(a). This could be due to the formation of the Sn-deficient and O-rich surface by the treatment.[6] When the Rh layer changed
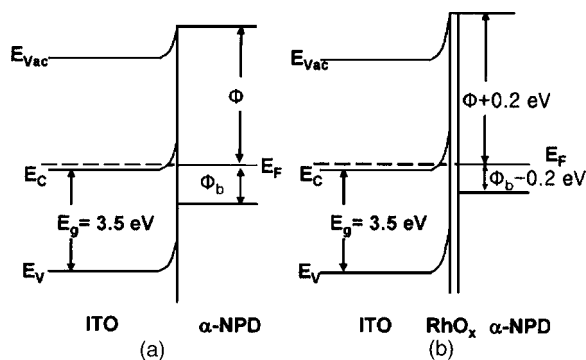

FIG. 5. Schematic band diagram: (a) O_2 plasma-treated ITO and (b) O_2 plasma-treated Rh layer on ITO.

to a transparent RhO_x layer by O_2 plasma treatment, the work function increased [Fig. 4(a)], leading to the increase in band bending, as shown in Fig. 5(b). The injection barrier for holes from anodes to organic materials corresponds to the energy difference between the work function of anodes and ionization energy of organic materials. Thus, the hole injection barrier of ITO, Φ_b, decreased to Φ_b-0.2 eV with O_2 plasma treatment. Therefore, the interfacial layer of RhO_x plays a role in lowering the potential barrier between ITO and organic materials, reducing the turn-on voltage of OLEDs.

In conclusion, we have reported the advantage of interfacial RhO_x layers between anodes of ITOs and hole transport layers of α-NPD on the electrical properties of OLEDs. The turn-on voltage of OLEDs decreased from 7 to 5 V and the operation voltage at 700 cd/m^2 decreased from 13 to 10 V as the RhO_x layer exists between ITO and α-NPD. The RhO_x layer had a higher work function than ITO by 0.2 eV. Thus, the RhO_x layer lowered the potential barrier for hole injection from ITO to α-NPD, reducing the turn-on voltage of OLEDs and increasing quantum efficiency.

[1] G. Liu, J. B. Kerr, and S. Johnson, Synth. Met. **144**, 1 (2004).
[2] L. S. Hung, C. W. Tang, and M. G. Mason, Appl. Phys. Lett. **70**, 13 (1997).
[3] M. Y. Chan, S. L. Lai, M. K. Fung, S. W. Tong, C. S. Lee, and S. T. Lee, Appl. Phys. Lett. **82**, 1784 (2003).
[4] S.-F. Chen and C.-W. Wang, Appl. Phys. Lett. **85**, 765 (2004).
[5] S. W. Tong, C. S. Lee, Y. Lifshitz, D. Q. Gao, and S. T. Lee, Appl. Phys. Lett. **84**, 4032 (2004).
[6] K. H. Lee, H. W. Jang, K.-B. Kim, Y.-H. Tak, and J.-L. Lee, J. Appl. Phys. **95**, 586 (2004).
[7] I.-M. Chan and F. C. Hong, Thin Solid Films **450**, 304 (2004).
[8] C.-M. Hsu and W.-T. Wu, Appl. Phys. Lett. **85**, 840 (2004).
[9] D. R. Lide, *CRC Handbook of Chemistry and Physics*, 83rd ed. (CRC Press, Boca Raton, FL, 2002).
[10] D. Y. Noh, Y. Hwu, H. K. Kim, and M. Hong, Phys. Rev. B **51**, 4441 (1995).
[11] L. Chkoda, C. Heske, M. Sokolowski, E. Umbach, F. Steuber, J. Staudigel, M. Stobel, and J. Simmerer, Synth. Met. **111**, 315 (2000).
[12] W. R. Salaneck, N. Johansson, K. Z. Xing, F. Cacialli, R. H. Friend, G. Beamson, and D. T. Clark, Synth. Met. **92**, 207 (1998).
[13] D. J. O'Connor, B. A. Sexton, and R. St. C. Smart, *Surface Analysis Methods in Materials Science* (Springer-Verlag, Berlin, 1992).
[14] J. F. Moulder, W. F. Strickle, P. E. Sobol, and K. D. Bomben, *Handbook of X-Ray Photoelectron Spectroscopy* (Perkin-Elmer, Eden Prairie, MN, 1992).
[15] J. M. Baik and J.-L. Lee, Met. Mater. Int. **10**, 555 (2004).
[16] A. K. Kulkarni and S. A. Knickerbocker, J. Vac. Sci. Technol. A **14**, 1709 (1996).